Molecular Biology of the Cell
Vol. 20, 3763–3771, August 15, 2009

The Role of the Exocyst in Matrix Metalloproteinase Secretion and Actin Dynamics during Tumor Cell Invadopodia Formation

Jianglan Liu,* Peng Yue,* Vira V. Artym,†‡ Susette C. Mueller,† and Wei Guo*

*Department of Biology, University of Pennsylvania, Philadelphia, PA 19104-6018; †Department of Oncology, Lombardi Comprehensive Cancer Center, Georgetown University Medical School, Washington, DC 20057-1469; and ‡Laboratory of Cell and Developmental Biology, National Institute of Dental and Craniofacial Research, National Institutes of Health, Bethesda, MD 20892-4370

Submitted September 23, 2008; Revised June 5, 2009; Accepted June 9, 2009
Monitoring Editor: Jean E. Schwarzbauer

Invadopodia are actin-rich membrane protrusions formed by tumor cells that degrade the extracellular matrix for invasion. Invadopodia formation involves membrane protrusions driven by Arp2/3-mediated actin polymerization and secretion of matrix metalloproteinases (MMPs) at the focal degrading sites. The exocyst mediates the tethering of post-Golgi secretory vesicles at the plasma membrane for exocytosis and has recently been implicated in regulating actin dynamics during cell migration. Here, we report that the exocyst plays a pivotal role in invadopodial activity. With RNAi knockdown of the exocyst component Exo70 or Sec8, MDA-MB-231 cells expressing constitutively active c-Src failed to form invadopodia. On the other hand, overexpression of Exo70 promoted invadopodia formation. Disrupting the exocyst function by si*EXO70* or si*SEC8* treatment or by expression of a dominant negative fragment of Exo70 inhibited the secretion of MMPs. We have also found that the exocyst interacts with the Arp2/3 complex in cells with high invasion potential; blocking the exocyst-Arp2/3 interaction inhibited Arp2/3-mediated actin polymerization and invadopodia formation. Together, our results suggest that the exocyst plays important roles in cell invasion by mediating the secretion of MMPs at focal degrading sites and regulating Arp2/3-mediated actin dynamics.

INTRODUCTION

A key feature of cancer is the ability of the tumor cells to break through tissue barriers and invade into surrounding tissues. The initial step of tumor cell invasion is the formation of cell protrusions in the direction of cell movement. Invadopodia are specialized membrane protrusions formed by invading tumor cells that extend into the extracellular matrix (ECM). At the ultrastructural level, invadopodia are filament-like extensions from the ventral surface of the cells adherent to matrix that range from 8 to 10 μm in diameter and reach more than 2 μm in length (Buccione *et al.*, 2004; Marx, 2006; Linder, 2007). Time-lapse image analysis has shown that invadopodia are formed de novo at the cell periphery and their lifetime varies from minutes to several hours (Yamaguchi *et al.*, 2005). Invadopodial protrusions are actin-based structures enriched in actin-associated proteins, adhesion proteins, matrix proteases such as matrix metalloproteinases (MMPs) and signaling proteins that regulate the actin cytoskeleton and membrane remodeling. However, how multiple processes including signaling, protease secretion, and actin assembly are coordinated to produce a functional ECM-degrading machine remains poorly understood.

Focal degradation of tissue barriers by MMPs plays a critical role in tumor invasion. The matrix-degrading capability of invadopodia is largely dependent on MMPs, including MT1-MMP, MMP-2, and MMP-9 (Gimona and Buccione, 2006; Linder, 2007). MT1-MMP is a transmembrane protease essential for invadopodial activity (Itoh and Seiki, 2006). MMP-2 was the first MMP found to localize at invadopodia of Src-transformed fibroblasts (Monsky *et al.*, 1993). MMP-9 was also found at invadopodial structures such as those of the metastatic breast cancer cells (Bourguignon *et al.*, 1998) and leukemia cells (Redondo-Muñoz *et al.*, 2006). The secretion of a combination of MMPs is important for effective invasion. However, the exact mechanism by which MMPs are targeted to and exocytosed at invadopodia-forming sites is unclear.

In addition to MMP secretion, the formation of cell protrusions also involves the assembly of branched actin filaments at the leading edge. The Arp2/3 complex is the core machinery that nucleates actin for the generation of branched filamentous actin networks. During invadopodia formation, the Arp2/3 complex has been shown to play a crucial role in the formation of degrading protrusions (Yamaguchi *et al.*, 2005). However, how actin assembly is controlled during invadapodia formation is still not well understood.

The exocyst is an evolutionarily conserved octameric protein complex that mediates the tethering of secretory vesicles to the plasma membrane for exocytosis (Guo *et al.*, 2000; Hsu *et al.*, 2004; Munson and Novick, 2006; He and Guo, 2009). The exocyst complex is involved in many cellular processes that require polarized exocytosis, including yeast budding, neurite extension, epithelia polarization, and cytokinesis (for review, see Hsu *et al.*, 2004). Here we hypothesize that the

This article was published online ahead of print in *MBC in Press* (http://www.molbiolcell.org/cgi/doi/10.1091/mbc.E08–09–0967) on June 17, 2009.

Address correspondence to: Wei Guo (guowei@sas.upenn.edu).

exocyst is involved in invadopodial activities via regulating the secretion of MMPs at the focal degradation sites. Recently, the exocyst has also been shown to be involved in actin-based membrane protrusion and cell migration (Zuo *et al.*, 2006; Rosse *et al.*, 2006). The exocyst component, Exo70, directly interacts with the Arp2/3 complex, and this interaction is important for the regulation of actin assembly at the leading edge of migrating cells (Zuo *et al.*, 2006). Therefore it is likely that the exocyst also regulates actin dynamics during invadopodia formation through its interaction with the Arp2/3 complex.

Here, we report that the exocyst plays a pivotal role in invadopodial activity. We have found that blocking the exocyst function inhibits invadopodial formation. RNAi knockdown of the exocyst component Exo70 or Sec8 in MDA-MB-231 cells expressing mutant Y527F c-Src abolished the secretion of MMPs, whereas the overexpression of Exo70 promoted MMP secretion. In addition, the exocyst-Arp2/3 interaction is important for actin assembly during invadopodia formation. Together, these findings suggest that the exocyst coordinates protease secretion and cytoskeleton dynamics during tumor invasion.

MATERIALS AND METHODS

Plasmids and Antibodies

Full-length rat Exo70 (rExo70 FL) cDNA was cloned in-frame in pEGFP-C1 and pJ3-GFP vectors for expression as enhanced green fluorescent protein (EGFP) or GFP fusions. Exo70ΔC (amino acids 1-408) was cloned in-frame in pEGFP-C1. The *exo70* mutant, Exo70$^{\Delta 628-630}$, was generated using the QuikChange site-directed mutagenesis kit (Stratagene, La Jolla, CA) with GFP-Exo70 in pEGFP-C1 as a template (Zuo *et al.*, 2006). Constructs were confirmed by restriction enzyme analysis and sequencing. Monoclonal antibodies against Exo70 and Sec8 were generously provided by Dr. Shu-Chan Hsu (Rutgers University, Piscataway, NJ). Mouse anti-actin mAb (MAB 1501, clone C4) was purchased from Chemicon, Millipore (Bedford, MA).

Cell Culture and RNA Interference Treatment

Human breast carcinoma MDA-MB-231 cells and stable lines of parental cells transfected with Y527F constitutively active c-Src were maintained at 37°C in DMEM (Invitrogen, Carlsbad, CA) supplemented with 10% FBS, 2 mmol/L L-glutamine, 100 U ml^{-1} penicillin, and 100 μg ml^{-1} streptomycin in a 5% CO_2 incubator. Cell transfections were carried out using Lipofectamine 2000 (Invitrogen, Carlsbad, CA). For RNA interference (RNAi), cells were grown to 50% confluence and transfected with small interfering RNA (siRNA) duplexes using Lipofectamine 2000. The human *EXO70(1)* siRNA target sequence is 5′-GGTTAAAGGTGACTGATTA-3′. The human *EXO70(2)* siRNA target sequence is 5′-GACCTTCGACTCCCTGATA-3′. The human *SEC8* siRNA target sequence is 5′- AGAACCTGCTTTCATGCAA-3′. The control Luciferase GL2 siRNA target sequence is 5′-AACGTACGCGGAATACTTCGA-3′. The efficiency of the knockdown was determined by Western blot.

Fluorescent Gelatin Degradation Assay

AlexaFluor 568–conjugated gelatin was prepared by labeling porcine gelatin (Sigma, St. Louis, MO) with AlexaFluor 568 (Molecular Probes, Eugene, OR) according to the manufacturer's instructions. Coverslips (18 mm) were precleaned with 20% nitric acid for 30 min followed by extensive washing and ethanol sterilization. The coverslips were coated with 50 μg/ml poly-L-Lysine (Sigma) for 20 min at room temperature, washed with PBS, and fixed with 0.5% glutaraldehyde (Ted Pella, Irvine, CA) for 15 min followed by extensive washing. The coverslips were then inverted on a drop of gelatin matrix (0.2% gelatin and AlexaFluor 568–labeled gelatin at an 8:1 ratio) and incubated for 10 min at room temperature. After washing with PBS, coverslips were incubated in 5 mg/ml sodium borohydride for 15 min, washed three times in PBS, and finally incubated in 2 ml of DMEM for 2 h before adding the cells.

To examine the ability of cells to form invadopodia and degrade matrix, 4×10^5 cells were plated on coverslips coated with AlexaFluor 568 and incubated at 37°C for 4 h. Cells were then fixed and prepermeabilized with 10% Formalin/0.1% Triton X-100 in PBS for 15 min at room temperature. After three washes, cells were postpermeabilized with 0.5% Triton X-100 for 5 min. Cells were then washed with PBS, labeled with primary antibodies for 2 h, and followed by labeling with secondary fluorochrome-conjugated antibodies for 1 h. Actin filaments were visualized with Alexa-phalloidin (Molecular Probes). Cells were imaged with the Leica DM IRB microscope (Deerfield, IL; 100×objective), a high-resolution CCD camera (model ORCA-ER, Hamamatsu Photonics, Bridgewater, NJ) and the Leica TCS SL laser-scanning confocal microscope (63x objective, Deerfield, IL). Images were processed with Adobe Photoshop (Adobe Systems, San Jose, CA; ver. 7.0). For quantification of degradation, percentage of cells with different degradation levels was calculated. Degradation levels of individual cells are reported as the total area of the degraded zones per cell relative to the area of the whole cell. The area of degraded matrix in the fields was measured using ImageJ 1.73v software (http://rsb.info.nih.gov/ij/). Dark spots on the bright, fluorescent gelatin matrix were inverted and thresholded into black dots on white background, followed by automatic outlining of the dots (Supplemental Figure S1). The area of the whole cell was measured by manually outlining the cell boundary (Supplemental Figure S1).

Zymography

The "in-gel" zymography was used for the detection of MMPs on the basis of their different molecular weights (Van den Steen *et al.*, 2002; Mott and Werb, 2004). After treatments, cells were cultured in serum-free DMEM for 48 h. Cell culture media were concentrated 50 times by filtration on Microcon concentrators (Millipore). Samples were mixed with SDS loading buffer (10% SDS, 50% glycerol, 0.4 M Tris, pH 6.8, and 0.1% bromophenol blue) and separated on 8% polyacrylamide/0.3% gelatin gels. Gels were then washed in 2.5% Triton X-100, 30 min each time, and incubated in reaction buffer (50 mM Tris, pH 8.0, and 5 mM $CaCl_2$) at 37°C for 24–48 h. After the reaction, gels were stained with staining buffer (0.12% Coomassie blue R-250, 50% methanol, and 20% acetic acid) for 1 h and destained overnight with destaining buffer (22% methanol and 10% acetic acid). Gels were scanned using CanoScan 4400F. Gel loadings were normalized to total protein measured with a Bio-Rad Protein Assay (Richmond, CA).

Glutathione S-Transferase-CA (Cofilin and Acidic Domains of N-WASP) Pulldown Assay

MDA-MB-231 parental and c-Src (Y527F)-transfected cells were lysed in the lysis buffer (20 mM Tris-HCl, pH 7.5, 25 mM KCl, 1 mM $MgCl_2$, 0.5 mM EGTA, 1 mM DTT, 0.5% Triton X-100, and protease inhibitors). A high-speed centrifugation (12,000 rpm, 15 min) was carried out, and 1 ml of precleared cell lysates (1.5 mg total protein) was mixed with 20 μl (50% vol/vol) of glutathione Sepharose conjugated with 10 μg glutathione *S*-transferase (GST)-CA (cofilin and acidic domains of N-WASP) proteins. After incubation at 4°C overnight, the beads were washed five times with the lysis buffer, and the bound proteins were analyzed by Western blot using antibodies against Exo70 and Arp3. GST alone was used as a negative control in the experiment.

Pyrene Actin Assay

Cell lysates were collected in buffer B (20 mM Tris-HCl, pH 7.5, 25 mM KCl, 1 mM $MgCl_2$, 0.5 mM EGTA, 0.1 mM ATP, and protease inhibitor cocktail [Sigma P8340, 4-(2-aminoethyl) benzenesulfonyl fluoride, pepstatin A, E-64, bestatin, leupeptin, and aprotinin], and 1 mM DTT) and spun successively at 16,000 × *g* for 15 min and 80,000 rpm in a Beckman TLA-100.3 rotor (Fullerton, CA) for 20 min at 4°C. The resulting high-speed supernatant (HSS) was used for later experiments. Pyrenyl-actin was dissolved in column buffer (TEA, 0.3 mM $CaCl_2$, 0.1 mM EDTA, 0.7 mM ATP, and 6.25 mM NaN_3) for 1 h, spun at 80,000 rpm in a Beckman TLA-100.3 rotor for 20 min at 4°C to remove F-actin, and mixed with Mg^{2+} converting buffer for 5 min to convert Ca^{2+}-actin to Mg^{2+}-actin. Mg^{2+}-pyrenl-actin was then diluted in the polymerization buffer (60 mM KCl, 2.5 mM NaCl, 0.6 mM $MgCl_2$, 5 mM Tris-HCl, pH 7.5, 2.5 mM HEPES, pH 7.1, 0.5 mM EGTA, 30 μM $CaCl_2$, 0.2 mM ATP, and 0.3 mM NaN_3) to a final concentration of 1.5 μM and immediately mixed with HSS, which contained 2.4–2.6 μM unlabeled G-actin as estimated by Western blot (data not shown) in the presence of 0.2 mM ATP and 50 nM GST-tagged verprolin, cofilin, and acidic (VCA) domain of mammalian N-WASP. The mixture was quickly transferred into a cuvette, and the fluorescence intensity was read every 5 s in a fluorometer. Three independent measurements were carried out for each treatment. Polymerization curves and rates were obtained using Excel (Microsoft, Redmond, WA). The polymerization rate was represented as the maximal slope of the elongation phase of each curve, and the normalized polymerization rate was calculated as the rate of each treatment relative to the control treatments. Each polymerization curve was first smoothed using Sigmaplot software to elicit trends from noisy data. Then the slope of each point on the curve was calculated as the slope of the line between this point and the point 60 s ahead. The slopes of all the points on each curve were used to create a new plot. The maximal value of this slope curve is regarded as the actin polymerization rate.

RESULTS

The Exocyst Is Necessary for Invadopodial Activity

A matrix degradation assay was used to study invadopodia formation. This assay involves culturing cells on coverslips coated with thin, fluorochrome-conjugated gelatin matrices. Local proteolytic activity was identified by the appearance of dark areas lacking fluorescence in the bright fluorescent

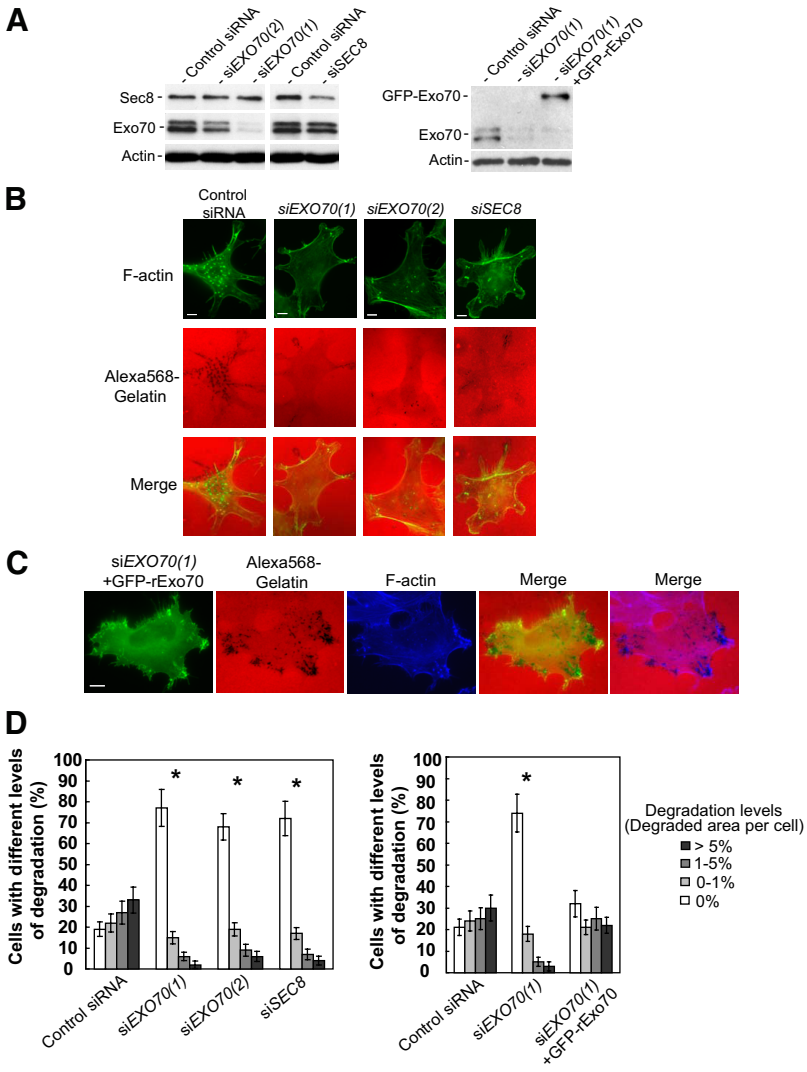

Figure 1. Knockdown of the exocyst inhibits invadopodial activity. (A) Expression levels of the exocyst subunits Exo70 and Sec8 in MDA-MB-231 (Y527F c-Src) cells transfected with siRNAs. Lysates were prepared from cells transfected with siRNA oligos targeting Luciferase (Control siRNA), Exo70 (two different oligos: si*EXO70(1)* and si*EXO70(2)*), or Sec8 (si*SEC8)*. siRNA treatments led to significant reduction in the amounts of Exo70 and Sec8 in the cells. The levels of Exo70 and Sec8 in cell lysates were analyzed by Western blot (left panel). In the rescue experiment, si*EXO70(1)* knockdown cells were transfected with GFP-tagged rat Exo70 (GFP-rExo70). The amounts of endogenous Exo70 and GFP-rExo70 were detected by Western blot (right panel). The amounts of actin were also examined as loading controls. (B) MDA-MB-231 (Y527F c-Src) cells with RNAi knockdown were cultured on Alexa 568–labeled gelatin film for 4 h. Cells were then fixed and stained with phalloidin-Alexa 488 to label F-actin. Individual and merged images of F-actin (green) and gelatin (red) were shown. RNAi knockdown of Exo70 or Sec8 decreased the amount of focal degradation (the black dots). (C) Gelatin degradation assay was performed in si*EXO70(1)* knockdown cells expressing GFP-rExo70. Individual and merged images of GFP-rExo70 fluorescence (green), F-actin (blue), and gelatin (red) are shown. The expression of GFP-rExo70 in si*EXO70(1)* knockdown cells rescued invadopodia formation in these cells. (D) Comparison of focal degradation in cells with exocyst knockdown. Four independent measurements (50 cells each) for each siRNA treatment (left panel) and rescue experiment (right panel) were carried out. Error bars, SD. *$p < 0.01$. Scale bar, 5 μm.

matrix (Artym *et al.*, 2006). MDA-MB-231 parental cells were used in the experiments, along with cells stably transfected with the constitutively active c-Src (Y527F c-Src), which have increased invasive potential.

To examine the role of the exocyst in invadopodia formation, we examined the effect of siRNA-mediated knockdown of endogenous exocyst subunits on invadopodia formation in c-Src–activated cells. Using different siRNA oligos that target *EXO70* (si*EXO70(1)* and si*EXO70(2)*) and *SEC8* (si*SEC8*), we observed effective knockdown of the target proteins by Western blot (82% for si*EXO70(1)*, 67% for si*EXO70(2)* and 69% for si*SEC8* (Figure 1A, left panel). The knockdown cells formed much fewer invadopodia as indicated by fewer matrix degradation sites and a smaller matrix degradation area. Correspondingly, the number of actin puncta localized to sites of matrix degradation was also reduced in the knockdown cells (Figure 1B). We have also examined whether the expression of rat Exo70 is able to rescue the defect of invadopodia formation in si*EXO70*-treated MDA-MB-231 (Y527F c-Src) cells. Rat Exo70 is more than 90% identical in amino acid sequence to human Exo70, yet it is not targeted by the human *EXO70* siRNA oligonucleotides used in this study. The level of Exo70 knockdown and the expression of GFP-rExo70 are shown in Figure 1A (right panel). We found that the defect of invadopodia formation in si*EXO70*-treated cells was rescued by the expression of rat Exo70 (Figure 1C). Quantification of the results from four independent experiments was carried out in si*EXO70*, si*SEC8*, control siRNA-treated cells, and si*EXO70*-treated cells expressing GFP-rExo70. The degradation level was calculated by dividing the total area of the degraded zones per cell by the area of the whole cell. Quantification of degradation levels was included in *Materials and Methods*, and representative photographs were shown in Supplemental Figure S1. The percentage of cells with different degradation levels was calculated for each treatment. As shown in Figure 1D, most of the *EXO70* or *SEC8* siRNA-treated cells did not form detectable invadopodia (77% for si*EXO70(1)*, 68% for si*EXO70(2)* and 72% for si*SEC8*), whereas most of the control siRNA-treated cells formed invadopodia (81%; left panel). The expression of rat Exo70 in si*EXO70(1)*-treated cells largely rescued the degradation defects in these cells. The percentage of cells that formed invadopodia was restored from 26% to 68%) (Figure 1D, right panel).

We have also examined whether the exocyst is able to induce the formation of invadopodia. As shown in Figure 2A, in the parental MDA-MB-231 cells, expression of GFP-tagged Exo70 led to increases in both the numbers of inva-

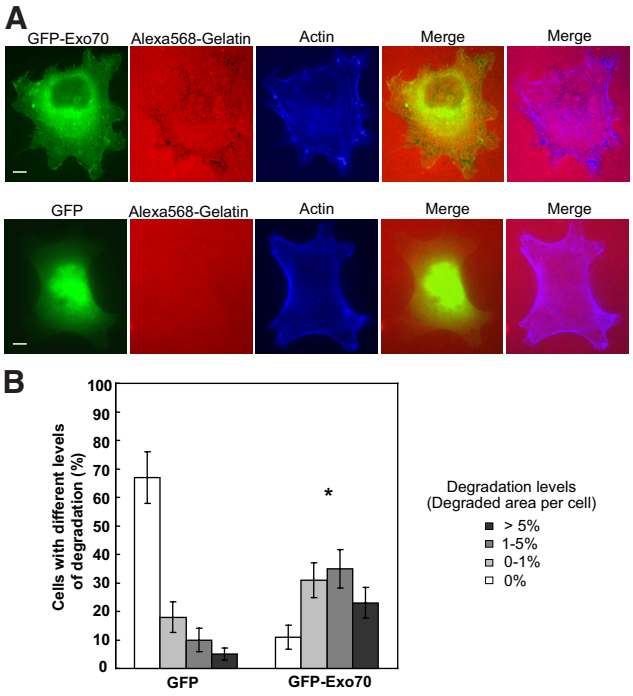

Figure 2. Overexpression of Exo70 stimulates invadopodial activity. (A) MDA-MB-231 cells were transfected with GFP-tagged Exo70 (GFP-Exo70), plated on fluorescent Alexa 568–labeled gelatin film for 4 h, and then processed for microscopy. Individual and merged images of GFP-Exo70 fluorescence (green), F-actin (blue), and gelatin (red) are shown. Overexpression of GFP-Exo70 stimulated focal degradation in MDA-MB-231 cells (top panel). Cells transfected with GFP alone were used as negative control (bottom panel). (B) Quantification of degradation areas in cells overexpressing Exo70. Three independent measurements (~70 cells each) for each treatment were carried out. Error bars, SD. *$p < 0.01$. Scale bar, 5 μm.

dopodia and areas of degradation in each transfected cell, whereas expression of GFP alone did not cause any change in invadopodia formation (data not shown). The percentage of cells with different degradation levels in GFP-Exo70 and control vector-transfected cells was quantified. As shown in Figure 2B, the percentage of cells with focal matrix degradation was substantially increased in Exo70-transfected cells (31, 35, and 23% for 0–1, 1–5, and >5% degradation levels, respectively) compared with control cells (18, 10, and 5% for 0–1, 1–5, and >5% degradation levels, respectively). We also examined whether the exocyst is able to induce the formation of invadopodia in Y527F c-Src–expressing cells. As shown in Supplemental Figure S2, expression of GFP-tagged Exo70 further promoted invadopodia formation in transfected cells. Expression of GFP alone was used as a negative control. Collectively, these results suggest that the exocyst plays a crucial role in invadopodia formation and invasion.

We also noticed that cells transfected with siRNA against Exo70 have weaker F-actin staining comparing with control cells or Sec8 siRNA-treated cells. The effect of Exo70 on actin organization will be discussed later.

The Localization of the Exocyst at Invadopodia-forming Sites

Next, we examined the localization of exocyst components in the parental MDA-MB-231 cells using confocal microscopy. In addition to the staining in the cytosol, endogenous Exo70 was also enriched in invadopodia as well as the plasma membrane (Figure 3A). Part of the Exo70 staining colocalized with actin puncta at sites of matrix degradation. We have also examined the localization of GFP-tagged Exo70, expressed at low levels using the pJ3-GFP vector, in MDA-MB-231 cells. As shown in Figure 3B, there are partial overlaps of Exo70 and the degrading foci. Sec8 has a similar pattern of localization to the invasion sites (data not shown; Sakurai-Yageta *et al.*, 2008). The exocyst components were not always enriched at the degradation sites. This may be due to the highly dynamic nature of invadopodia and the mobility of the cells. Indeed, as previously demonstrated, F-actin and its regulatory proteins were not always detected at sites of degradation (Artym *et al.*, 2006). It is possible that the localization of the exocyst at invadopodia-forming sites is transient. Some of the focal degradation sites may represent regions where the exocyst completed their function.

The Exocyst Is Required for the Secretion of MMPs in MDA-MB-231 (Y527F c-Src) Cells

The exocyst mediates the tethering of secretory vesicles at the plasma membrane for exocytosis. It is thus likely that the exocyst mediates the secretion of MMPs at invadopodial sites. To test this hypothesis, we examined the effect of siRNA knockdown of *EXO70* and *SEC8* on the secretion of MMP-2 and MMP-9 in MDA-MB-231 (Y527F c-Src) cells. Substrate zymography was used to detect the secretion levels of MMP-2 and MMP-9. Gelatin zymography analyses of cell culture media detected a significant decrease in the levels of MMP-2 and MMP-9 in both *EXO70* and *SEC8* knockdown cells (Figure 4A). We have also examined whether the expression of rat Exo70 is able to rescue the secretion defect in si*EXO70*-treated MDA-MB-231 (Y527F c-Src) cells. The expression of rat Exo70 did not affect *EXO70* siRNA knockdown efficiency on endogenous Exo70 (Figure 4A). We found that the MMP secretion defects in si*EXO70(1)*-treated cells was rescued by the expression of rat Exo70 (Figure 4A). In all treatments, quantification of secreted MMP levels was performed based on three independent experiments for each group. The levels of secreted MMP were represented as normalized secretion index, which was calculated as the percentage of secreted MMP relative to that of the control cells. As shown in Figure 4B, in *EXO70* and *SEC8* siRNA-treated cells, secretion of MMP-2 decreased to 8% for si*EXO70(1)*, 18% for si*EXO70(2)*, and 17% for si*SEC8*; secretion of MMP-9 decreased to 10% for si*EXO70(1)*, 19% for si*EXO70(2)*, and 18% for si*SEC8*. The expression of rat Exo70 in si*EXO70*-treated cells largely rescued the secretion defect of MMPs in these cells (72% for MMP-2 and 81% for MMP-9). These findings strongly suggest that the exocyst complex is essential for the secretion of the key invadopodia-associated MMPs.

We have previously shown that Exo70 directly interacts with phosphatidylinositol 4,5-bisphosphate ($PI(4,5)P_2$) through its C-terminus, and that this interaction is critical for the association of Exo70 with the plasma membrane and the targeting of post-Golgi secretory vesicles to the plasma membrane (He *et al.*, 2007; Liu *et al.*, 2007). Disrupting the interaction between Exo70 and the plasma membrane by overexpressing a C-terminal truncated version of Exo70 (GFP-Exo70ΔC, a.a. 1-408) would be expected to inhibit the secretion of MMPs. As shown in Figure 5, A and B, expression of Exo70ΔC caused a dramatic decrease in the amounts of MMP-2 and MMP-9 secreted in the medium (81% decrease for MMP-2 and 82% decrease for MMP-9) compared with GFP-transfected cells. We also examined whether the overexpression of full-length Exo70 (GFP-Exo70) is able to promote the secretion of MMPs. Gelatin zymography de-

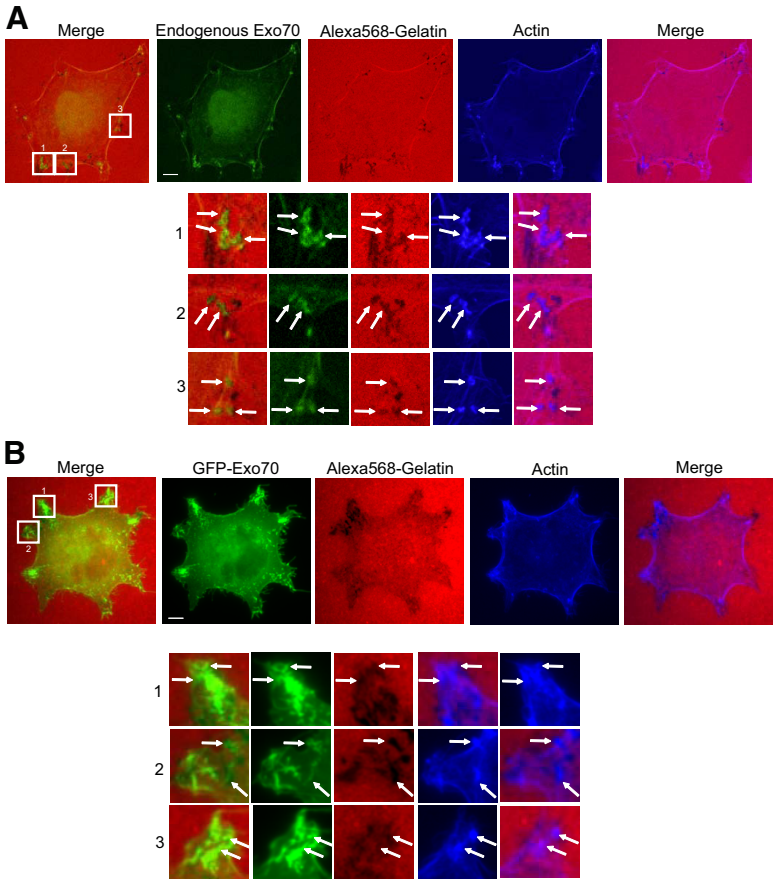

Figure 3. Localization of Exo70 at the focal degradation sites. (A) MDA-MB-231 cells were plated on fluorescent Alexa 568–labeled gelatin (red) for 20 h. After fixation, cells were stained for Exo70 (green). Individual and merged images are shown. Endogenous Exo70 showed colocalization with the "degradation holes" in the fluorescent gelatin matrix, along with some enrichment at the plasma membrane. (B) The localization of GFP-tagged Exo70 expressed at low levels using the pJ3-GFP vector was examined in MDA-MB-231 cells. GFP-tagged Exo70 partially overlapped with the degrading spots. Higher magnification views of the boxed areas are shown underneath each image. Arrows, colocalization of Exo70 and invadopodia-forming sites. Scale bars, 5 μm.

tected elevated levels of secreted MMP-2 (1.6-fold) and MMP-9 (1.7-fold) in cells expressing GFP-Exo70 (Figure 5, A and B). The observation that overexpression of Exo70ΔC led to reduced level of secreted MMPs suggests that the plasma-membrane targeting of the exocyst is crucial for the secretion of MMPs.

The Interaction between Exo70 and the Arp2/3 Complex is Required for Invadopodia Formation

Invadopodia formation involves membrane protrusions driven by Arp2/3-mediated actin polymerization (Yamaguchi *et al.*, 2005). Studies from our lab have shown that Exo70 directly interacts with the Arpc1 subunit of the Arp2/3 complex and that this interaction is important for actin-based membrane protrusion and cell motility (Zuo *et al.*, 2006). To investigate whether the exocyst-Arp2/3 interaction also plays a role in invadopodial activity, we first examined this interaction in carcinoma cells with different levels of invasiveness. It has been well demonstrated that the CA domain from the WASP family proteins binds to the Arp2/3 complex. We then used a recombinant GST-CA fusion protein to pull down the Arp2/3 complex from cells with various levels of invasiveness (HeLa cells, the parental MDA-MB-231 cells, and the Y527F c-Src cells) and examined the association of the exocyst with Arp2/3 in these cells. As shown in Figure 6A, a much greater amount of Exo70 was pulled down by GST-CA from Y527F c-Src cells than from parental MDA-MB-231 cells, and less Exo70 was pulled down from HeLa cells than from parental MDA-MB-231 cells. As a control, similar amounts of Arp3 were pulled down. On the other hand, neither Arp3 nor Exo70 was pulled down by GST. In addition, we did not detect any direct interaction between Exo70 and CA or VCA (Supplemental Figure S3). This observation indicated that the Exo70-Arp2/3 interaction was much stronger in Y527F c-Src cells than in parental MDA-MB-231 cells. As the Y527F c-Src cells are more invasive because of Src activation, this result suggests that the exocyst-Arp2/3 interaction is up-regulated in cells with high invasive potential.

We have previously shown that the *exo70* mutant, Exo70$^{\Delta 628-630}$, is specifically defective in interacting with the Arp2/3 complex (Zuo *et al.*, 2006). We thus tested whether the overexpression of Exo70$^{\Delta 628-630}$ would affect invadopodia formation. As shown in Figure 6B, overexpression of GFP-tagged Exo70$^{\Delta 628-630}$ (GFP-Exo70$^{\Delta 628-630}$) in Y527F c-Src cells largely inhibited matrix degradation, whereas transfection with GFP did not affect invadopodia formation. The percentage of cells without any invadopodia was significantly increased in Exo70$^{\Delta 628-630}$-transfected cells (Figure 6C, 66% for GFP-Exo70$^{\Delta 628-630}$-transfected cells and 22% for GFP-transfected cells). Overall, the above results suggest that the interaction between the exocyst and the Arp2/3 complex plays an important role in the formation of invadopodia.

Next, we directly tested whether Exo70 affects Arp2/3-mediated actin polymerization in cell lysates using pyrene actin assay (Kouyama and Mihashi, 1981). The lysates of Y527F c-Src cells with various siRNA treatments were collected and mixed with pyrenyl-actin in the presence of the VCA domain of mammalian N-WASP. siRNA knockdown efficiency as well as the amounts of actin and Arp2/3 in cell lysates was examined in all siRNA-treated samples (Figure

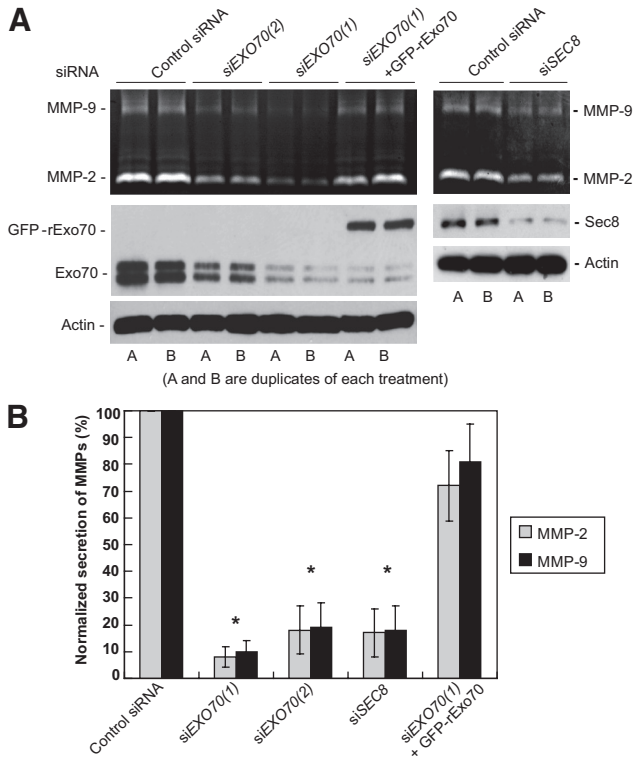

Figure 4. The exocyst is required for the secretion of MMPs in MDA-MB-231 (Y527F c-Src) cells. (A) Secretion of MMP-2 and MMP-9 was examined in MDA-MB-231 (Y527F c-Src) cells with Exo70 or Sec8 RNAi knockdown. Cell culture media were collected and concentrated. MMP-2 and MMP-9 activities were analyzed by gelatin zymography. Knockdown of Exo70 or Sec8 led to dramatic decreases of MMP-2 and MMP-9 secreted in the media (top panel). Expression of rat Exo70 rescued MMP secretion in Exo70 knockdown cells (si*EXO70(1)* + rExo70). The amounts of endogenous Exo70 and Sec8, and the amount of extragenically expressed GFP-tagged rat Exo70 were detected by Western blot using anti-Exo70 and Sec8 monoclonal antibodies (middle panel). Actin was used as the loading control (bottom panel). A and B are duplicates of each experiment. (B) Quantification of secreted MMP levels was performed based on three independent experiments for each group. Secreted MMPs were represented as normalized secretion index, which was calculated as the amount of secreted MMP relative to that of the control cells. Error bars, SD. *$p < 0.01$.

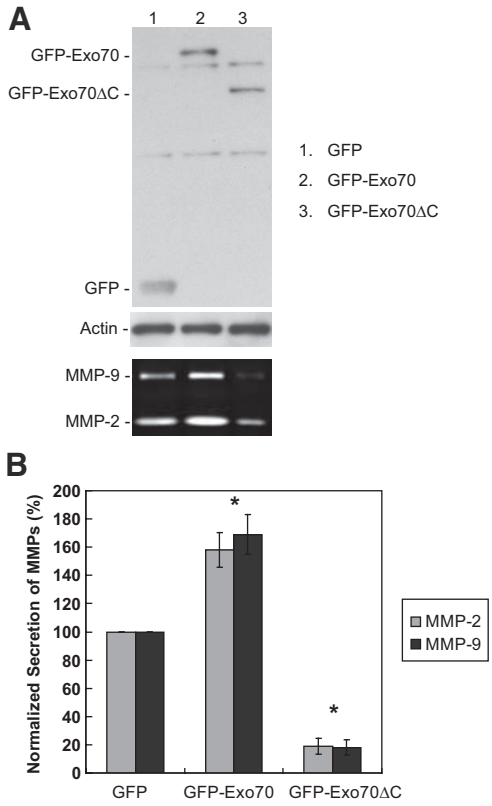

Figure 5. Zymography analyses of MMP-2 and MMP-9 secreted from MDA-MB-231 (Y527F c-Src) cells overexpressing Exo70ΔC (amino acids 1–408) or full-length Exo70. (A) After transfection with GFP-tagged Exo70ΔC or Exo70 for 18 h, cell culture media were collected and analyzed by gelatin zymography. Overexpression of Exo70ΔC caused a dramatic decrease in the amounts of MMP-2 and MMP-9 secreted in the media. Overexpression of Exo70 stimulated the secretion of MMPs (bottom panel). Cell lysates were collected for the detection of extragenically expressed GFP-tagged Exo70 proteins (top panel). Actin staining was shown as a loading control (middle panel). (B) Quantification of MMP secretion. Error bars, SD. *$p < 0.01$.

7A). Similar amounts of actin and Arp3 were observed for all the samples. As shown in Figure 7B, actin polymerization was inhibited in lysates from Exo70 knockdown cells compared with control siRNA-treated cells, as revealed by longer lag phase and decreased actin polymerization rate. As a control, cell lysates had little actin polymerization activity in the absence of VCA. *SEC8* siRNA-treated cells had a much smaller effect on actin assembly. We also examined the final levels of actin polymerization in all siRNA-treated samples after 24 h. As shown in Supplemental Figure S4A, the final level of actin polymerization is similar among all the samples. Moreover, we checked the amount of available actin in each reaction. As shown in Supplemental Figure S4B, the amounts of actin in the pellet (polymerizable actin) and supernatant (unpolymerizable actin) fractions were at the same level in each treatment. This result suggests that the differences in initial actin polymerization rates are not likely due to the difference in the levels of polymerization-competent actin. Quantification was carried out based on normalized polymerization rate. Polymerization rate was represented as the slope of the linear approximation line of each curve, and the normalized polymerization rate was calculated as the rate of each treatment relative to control siRNA-treated cells. As shown in Figure 7C, *EXO70* siRNA treatment decreased the normalized polymerization rate by more than two fold compared with control siRNA treatment.

We also tested whether overexpression of Exo70 promotes Arp2/3-mediated actin polymerization in cell lysates. As shown in Figure 7, E and F, lysates from cells overexpressing GFP-Exo70 showed a decreased lag phase and an increased actin polymerization rate compared with GFP-transfected cells (1.38-fold that of GFP-transfected cells). In contrast, lysates from cells overexpressing the Arp2/3 binding-deficient mutant of Exo70, GFP-Exo70$^{\Delta 628-630}$, had an increased lag phase and a lower actin polymerization rate compared with control cells (Figure 7, E and F, with a normalized polymerization rate of 0.52). The final levels of actin polymerization were identical in Exo70 overexpression samples (Supplemental Figure S4, A and B). The amounts of actin and Arp3 were similar for all the samples (Figure 7D). Collectively, these results suggest that Exo70 plays a positive regulatory

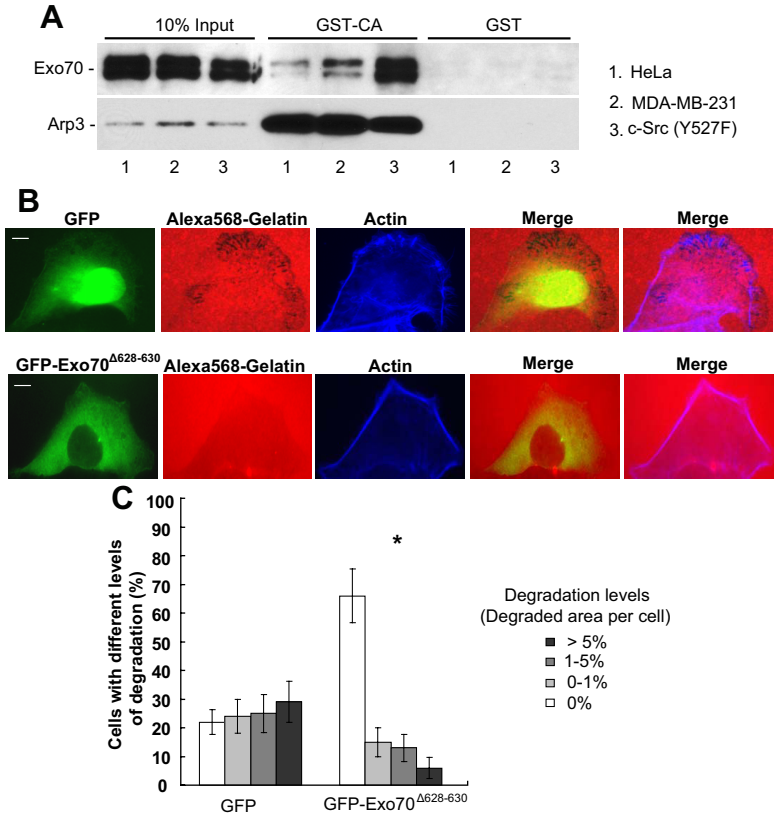

Figure 6. The interaction between Exo70 and the Arp2/3 complex is required for invadopodia formation. (A) The interaction between Exo70 and the Arp2/3 complex was examined in cells with different levels of invasiveness. GST-CA pulldown assay was performed in HeLa cells, MDA-MB-231 parental and c-Src (Y527F)-transfected cells as described in *Materials and Methods*. Although GST–CA–Sepharose (the CA domain of N-WASP) pulled down similar amounts of Arp2/3 in HeLa, MDA-MB-231 parental and c-Src (Y527F)-transfected cells, more Exo70 bound to Arp2/3 in c-Src (Y527F)-transfected cells than in MDA-MB-231 parental cells and less Exo70 bound to Arp2/3 in HeLa cells than in MDA-MB-231 parental cells. The inputs and the bound Exo70 and Arp2/3 were analyzed by Western blot using anti-Exo70 monoclonal and anti-Arp3 polyclonal antibodies, respectively. GST alone was used as a negative control in the binding assay. (B) Matrix degradation assay was performed in MDA-MB-231 (Y527F c-Src) cells transfected with GFP-tagged Exo70$^{\Delta 628-630}$ or GFP alone. After transfection with GFP-tagged Exo70$^{\Delta 628-630}$ or GFP for 18 h, cells were cultured on Alexa 568–labeled gelatin for 4 h and then processed for microscopy. Individual and merged images of GFP-Exo70 fluorescence (green), F-actin (blue), and gelatin (red) were shown. Overexpression of GFP-tagged Exo70$^{\Delta 628-630}$ in Y527F c-Src cells largely inhibited matrix degradation, whereas transfection with GFP did not affect invadopodia formation. (C) Quantification of percentages of cells with different degradation levels in each treatment in B. Error bars, SD. *$p < 0.01$.

role in Arp2/3-mediated actin polymerization in addition to its function in vesicle tethering and exocytosis during invadopodia formation.

DISCUSSION

Invadopodia are actin-based membrane protrusions formed by tumor cells that degrade the extracellular matrix for invasion. Investigation of the molecular mechanisms of invadopodia formation and regulation is important for the understanding of tumor invasion and metastasis. Here, we demonstrate that the exocyst plays a key role in invadopodia formation and invasion. The exocyst is enriched at focal degrading sites, and inhibition of its function leads to a reduction of invadopodial activity.

Focal degradation of the ECM barrier is a key feature of invadopodia, which is achieved by the secretion of proteases that degrade the basement membrane surrounding the tumor. A number of MMPs, including MMP-2 and MMP-9, have been shown to play an important role in degrading ECM during tumor invasion (Boyd, 1996; Chen, 1996; Chen and Wang, 1999; Deryugina and Quigley, 2006; Itoh and Seiki, 2006; Furmaniak-Kazmierczak *et al.*, 2007). MMPs are delivered to the surface of the tumor cells through exocytosis, and components of membrane traffic machinery have been implicated in tumorigenesis (Palmer *et al.*, 2002; Cheng *et al.*, 2004; Steffen *et al.*, 2008; Sakurai-Yageta *et al.*, 2008). The exocyst is involved in tethering post-Golgi secretory vesicles to the plasma membrane for exocytosis. Here, using RNAi and dominant-negative mutants to inhibit exocyst function, we demonstrate that the exocyst is required for the secretion of MMP-2 and MMP-9. Our results are also in agreement with recent study showing the involvement of the exocyst in the secretion of MT1-MMP, a transmembrane protease that degrades ECM (Sakurai-Yageta *et al.*, 2008). Together, these results indicate that the exocyst mediates the secretion of different classes of MMPs during tumor invasion.

Although the principal function of the exocyst is to tether secretory vesicles for secretion, recent studies suggest that the exocyst is also involved in actin-based membrane protrusion. It was shown that RalA and RalB, members of the Ras family of small GTP-binding proteins, regulate exocyst function (Brymora *et al.*, 2001; Moskalenko *et al.*, 2002; Sugihara *et al.*, 2002; Polzin *et al.*, 2002), and the Ral-exocyst interaction induces filopodia formation through a mechanism that is independent of exocytosis (Sugihara *et al.*, 2002). The exocyst is involved in cell migration (Zuo *et al.*, 2006; Rosse *et al.*, 2006; Spiczka and Yeaman, 2008). Furthermore, Exo70 was found to directly interact with the Arpc1 subunit of the Arp2/3 complex; EGF, which promotes cell membrane protrusion, stimulates the interaction between Exo70 and the Arp2/3 complex in HeLa cells (Zuo *et al.*, 2006). The Arp2/3 complex is the core machinery that nucleates actin for the generation of the branched actin network underneath the leading edges of the plasma membrane for membrane protrusion (Pollard and Borisy, 2003). It has been well established that the Arp2/3 complex is essential for invadopodia formation (Buccione *et al.*, 2004; Lorenz *et al.*, 2004; Yamaguchi *et al.*, 2005). RNAi-mediated knockdown of members of the Arp2/3 complex or N-WASP, the activator of Arp2/3, inhibited invadopodia formation (Lorenz *et al.*, 2004; Yamaguchi *et al.*, 2005). Microscopy analyses demonstrated that the Arp2/3 complex is enriched at invadopodia together with N-WASP (Yamaguchi *et al.*, 2005). Other regulators of the Arp2/3 complex such as Nck1, Cdc42, cortac-

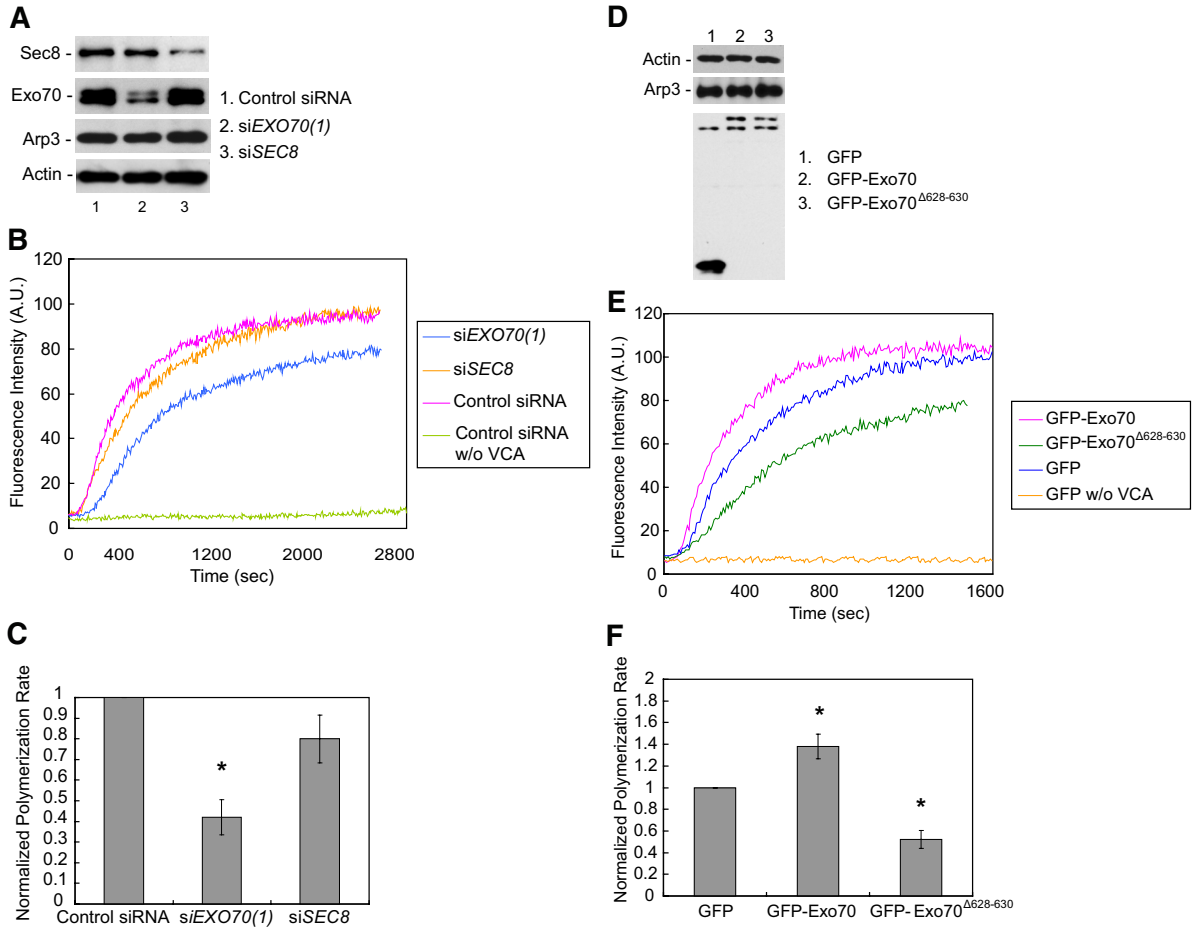

Figure 7. Exo70 is involved in Arp2/3-mediated actin polymerization in the cell. (A) Lysates were prepared from MDA-MB-231 (Y527F c-Src) cells transfected with indicated siRNA oligos. Exo70 and Sec8 knockdown levels were examined by Western blot, along with the amounts of actin and Arp3 in cell lysates. (B) The ability of the lysates to stimulate actin polymerization was analyzed by pyrene actin assay in the presence or absence of the VCA domain of N-WASP as described in *Materials and Methods*. The initial rate of actin polymerization, an indicator of actin nucleation by Arp2/3, was two fold lower in Exo70 knockdown cells than in the control cells. Sec8 knockdown slightly decreased the initial rate of actin polymerization. Cell lysates in the absence of VCA had little actin polymerization activity. (C) Normalized initial polymerization rates in each treatment in A were calculated by dividing the actin polymerization rate of each treatment by that of the control siRNA-treated cells. Three independent measurements for each treatment were carried out. Error bars, SD. *$p < 0.01$. ($n = 3$). (D) Actin polymerization kinetics was analyzed in lysates from MDA-MB-231 (Y527F c-Src) cells transfected with GFP-Exo70 and GFP-Exo70$^{\Delta 628-630}$ mutant. The levels of Exo70, actin, and Arp3 in cell lysates were detected by Western blot. (E) Lysates from cells expressing GFP-Exo70$^{\Delta 628-630}$ had a lower initial actin polymerization rate compared with GFP-transfected cells. Cells overexpressing GFP-Exo70 had an increased actin polymerization rate compared with the control cells. (F) Quantification of normalized polymerization rate of each treatment in D. Error bars, SD. *$p < 0.01$; $n = 3$.

tin, and WIP have also been shown to be involved in invadopodia formation (Yamaguchi *et al.*, 2005; Clark *et al.*, 2007). In the present study, we found that the exocyst has stronger interaction with the Arp2/3 complex in Src-activated cells compared with parental cells. Overexpression of the *exo70* mutant that is defective in its interaction with Arp2/3 inhibited invadopodia formation. How Src kinase regulates the Exo70-Arp2/3 interaction is still under investigation. Because GTPases such as Rac and Rho function downstream of Src kinase, these GTPases could be potential candidates for this process.

Using the pyrene actin assay, we have found that lysates from Y527F c-Src MDA-MB-231 cells are capable of stimulating Arp2/3-mediated actin polymerization in the presence of VCA. We further found that cells with Exo70 knockdown by RNAi or cells with overexpression of the *exo70* mutant deficient in Arp2/3-binding were less potent in Arp2/3-mediated actin polymerization, whereas lysates prepared from cells with Exo70 overexpression were more potent in stimulating actin polymerization. These data are consistent with the fluorescence microscope observation that there were fewer and dimmer F-actin foci in the Exo70 knockdown cells (Figure 1). These findings suggest that Exo70 plays a positive regulatory role in Arp2/3-mediated actin polymerization in cells. This is consistent with the observation that Exo70 overexpression led to extensive membrane protrusions in many types of cultured cells (Wang *et al.*, 2004; Xu *et al.*, 2005; Zuo *et al.*, 2006).

Overall, our study suggests that the exocyst is involved in invadopodia through mediating MMP secretion and regulating Arp2/3-mediated actin polymerization. The results suggest a coordination of protease secretion and cytoskeleton dynamics during tumor invasion. Future studies will focus on the molecular mechanisms by which Exo70 regulates actin dynamics and how the exocyst is regulated by upstream signaling molecules in the cell.

ACKNOWLEDGMENTS

We are grateful to Drs. Kenneth Yamada (National Institutes of Health), Henning Birkedal-Hansen (National Institutes of Health), Toshiyuki Yoneda (Osaka University), Shu-Chan Hsu (Rutgers University), Margaret Chou (University of Pennsylvania), Rytis Prekeris (University of Colorado), Jian Jing (University of Colorado), and Bing He (University of Pennsylvania) for reagents and constructive suggestions. This work is supported by grants from National Institute of General Medical Sciences and the Pew Scholars Program in Biomedical Sciences to W.G.

REFERENCES

Artym, V. V., Zhang, Y., Seillier-Moiseiwitsch, F., Yamada, K. M., and Mueller, S. C. (2006). Dynamic interactions of cortactin and membrane type 1 matrix metalloproteinase at invadopodia: defining the stages of invadopodia formation and function. Cancer Res. *66*, 3034–3043.

Bourguignon, L. Y., Gunja-Smith, Z., Iida, N., Zhu, H. B., Young, L. J., Muller, W. J., and Cardiff, R. D. (1998). CD44v(3,8–10) is involved in cytoskeleton-mediated tumor cell migration and matrix metalloproteinase (MMP-9) association in metastatic breast cancer cells. J. Cell. Physiol. *176*, 206–215.

Boyd, D. (1996). Invasion and metastasis. Cancer Metast. Rev. *15*, 77–89.

Brymora, A., Valova, V. A., Larsen, M. R., Roufogalis, B. D., and Robinson, P. J. (2001). The brain exocyst complex interacts with RalA in a GTP-dependent manner: identification of a novel mammalian Sec3 gene and a second Sec15 gene. J. Biol. Chem. *276*, 29792–29797.

Buccione, R., Orth, J. D., and McNiven, M. A. (2004). Foot and mouth: podosomes, invadopodia and circular dorsal ruffles. Nat. Rev. Mol. Cell Biol. *5*, 647–657.

Chen, W. T. (1996). Proteases associated with invadopodia, and their role in degradation of extracellular matrix. Enzyme Protein *49*, 59–71.

Chen, W. T., and Wang, J. Y. (1999). Specialized surface protrusions of invasive cells, invadopodia and lamellipodia, have differential MT1-MMP, MMP-2, and TIMP-2 localization. Ann. NY Acad. Sci. *878*, 361–371.

Cheng, K. W., *et al.* (2004). The RAB25 small GTPase determines aggressiveness of ovarian and breast cancers. Nat. Med. *10*, 1251–1256.

Clark, E. S., Whigham, A. S., Yarbrough, W. G., and Weaver, A. M. (2007). Cortactin is an essential regulator of matrix metalloproteinase secretion and extracellular matrix degradation in invadopodia. Cancer Res. *67*, 4227–4335.

Deryugina, E. I., and Quigley, J. P. (2006). Matrix metalloproteinases and tumor metastasis. Cancer Metastasis Rev. *25*, 9–34.

Furmaniak-Kazmierczak, E., Crawley, S. W., Carter, R. L., Maurice, D. H., Côté, G. P. (2007). Formation of extracellular matrix-digesting invadopodia by primary aortic smooth muscle cells. Circ. Res. *100*, 1328–1336.

Gimona, M., and Buccione, R. (2006). Adhesions that mediate invasion. Int. J. Biochem. Cell Biol. *38*, 1875–1892.

Guo, W., Sacher, M., Barrowman, J., Ferro-Novick, S., and Novick, P. (2000). Protein complexes in transport vesicle targeting. Trends Cell Biol. *10*, 251–255.

He, B., Xi, F., Zhang, X., Zhang, J., and Guo, W. (2007). Exo70 interacts with phospholipids and mediates the targeting of the exocyst to the plasma membrane. EMBO J. *26*, 4053–4065.

He, B., and Guo, W. (2009) The exocyst in polarized exocytosis. Curr. Opin. Cell Biol. 10.106/j.ceb.2009.04.007.

Hsu, S. C., TerBush, D., Abraham, M., and Guo, W. (2004). The exocyst complex in polarized exocytosis. Int. Rev. Cytol. *233*, 243–265.

Itoh, Y., and Seiki, M. (2006). MT1-MMP: a potent modifier of pericellular microenvironment. J. Cell. Physiol. *206*, 1–8.

Kouyama, T., and Mihashi, K. (1981). Fluorimetry study of N-(1-pyrenyl) iodoacetamide labelled F-actin. Eur. J. Biochem. *114*, 33–38.

Linder, S. (2007). The matrix corroded: podosomes and invadopodia in extracellular matrix degradation. Trends Cell Biol. *17*, 107–117.

Liu, J., Zuo, X., Yue, P., and Guo, W. (2007). Phosphatidylinositol 4,5-bisphosphate mediates the targeting of the exocyst to the plasma membrane for exocytosis in mammalian cells. Mol. Biol. Cell *18*, 4483–4492.

Lorenz, M., Yamaguchi, H., Wang, Y., Singer, R. H., and Condeelis, J. (2004). Imaging sites of N-WASP activity in lamellipodia and invadopodia of carcinoma cells. Curr. Biol. *14*, 697–703.

Marx, J. (2006). Podosomes and invadopodia help mobile cells step lively. Science *312*, 1868–1869.

Monsky, W. L., Kelly, T., Lin, C. Y., Yeh, Y., Stetler-Stevenson, W. G., Mueller, S. C., and Chen W. T. (1993). Binding and localization of M(r) 72,000 matrix metalloproteinase at cell surface invadopodia. Cancer Res. *53*, 3159–3164.

Moskalenko, S., Henry, D. O., Rosse, C., Mirey, G., Camonis, J. H., and White, M. A. (2002). The exocyst is a Ral effector complex. Nat. Cell Biol. *4*, 66–72.

Mott, J. D., and Werb Z. (2004). Regulation of matrix biology by matrix metalloproteinases. Curr. Opin. Cell Biol. *16*, 558–564.

Munson, M., and Novick, P. (2006). The exocyst defrocked, a framework of rods revealed. Nat. Struct. Mol. Biol. *13*, 577–581.

Palmer, R. E., Lee, S. B., Wong, J. C., Reynolds, P. A., Zhang, H., Truong, V., Oliner, J. D., Gerald, W. L., and Haber, D. A. (2002). Induction of BAIAP3 by the EWS-WT1 chimeric fusion implicates regulated exocytosis in tumorigenesis. Cancer Cell *2*, 497–505.

Pollard, T. D., and Borisy, G. G. (2003). Cellular motility driven by assembly and disassembly of actin filaments. Cell *112*, 453–465.

Polzin, A., Shipitsin, M., Goi, T., Feig, L. A., and Turner, T. J. (2002). Ral-GTPase influences the regulation of the readily releasable pool of synaptic vesicles. Mol. Cell. Biol. *22*, 1714–1722.

Redondo-Muñoz, J., Escobar-Díaz, E., Samaniego, R., Terol, M. J., García-Marco, J. A., and García-Pardo, A. (2006). MMP-9 in B-cell chronic lymphocytic leukemia is up-regulated by alpha4beta1 integrin or CXCR4 engagement via distinct signaling pathways, localizes to podosomes, and is involved in cell invasion and migration. Blood *108*, 3143–3151.

Rosse, C., Hatzoglou, A., Parrini, M. C., White, M. A., Chavrier, P., and Camonis, J. (2006). RalB mobilizes the exocyst to drive cell migration. Mol. Cell. Biol. *26*, 727–734.

Sakurai-Yageta, M., Recchi, C., Le Dez, G., Sibarita, J. B., Daviet, L., Camonis, J., D'Souza-Schorey, C., and Chavrier, P. (2008). The interaction of IQGAP1 with the exocyst complex is required for tumor cell invasion downstream of Cdc42 and RhoA. J. Cell Biol. *181*, 985–998.

Spiczka, K. S., and Yeaman, C. (2008) Ral-regulated interaction between Sec5 and paxillin targets Exocyst to focal complexes during cell migration. J. Cell Sci. *121*, 2880–2891.

Steffen, A., Le Dez, G., Poincloux, R., Recchi, C., Nassoy, P., Rottner, K., Galli, T., and Chavrier, P. (2008). MT1-MMP-dependent invasion is regulated by TI-VAMP/VAMP7. Curr. Biol. *18*, 926–931.

Sugihara, K., Asano, S., Tanaka, K., Iwamatsu, A., Okawa, K., and Ohta, Y. (2002). The exocyst complex binds the small GTPase RalA to mediate filopodia formation. Nat. Cell Biol. *4*, 73–78.

Van den Steen, P. E., Dubois, B., Nelissen, I., Rudd, P. M., Dwek, R. A., and Opdenakker, G. (2002). Biochemistry and molecular biology of gelatinase B or matrix metalloproteinase-9 (MMP-9). Crit. Rev. Biochem. Mol. Biol. *37*, 375–536.

Wang, S., Liu, Y., Adamson, C. L., Valdez, G., Guo, W., and Hsu, S. C. (2004). The mammalian exocyst, a complex required for exocytosis, inhibits tubulin polymerization. J. Biol. Chem. *279*, 35958–35966.

Xu, K. F., Shen, X., Li, H., Pacheco-Rodriguez, G., Moss, J., and Vaughan M. (2005). Interaction of BIG2, a brefeldin A-inhibited guanine nucleotide-exchange protein, with exocyst protein Exo70. Proc. Natl. Acad. Sci. USA *102*, 2784–2789.

Yamaguchi, H., *et al*. (2005) Molecular mechanisms of invadopodium formation: the role of the N-WASP-Arp2/3 complex pathway and cofilin. J. Cell Biol. *168*, 441–452.

Zuo, X., Zhang, J., Zhang, Y., Hsu, S. C., Zhou, D., and Guo, W. (2006). Exo70 interacts with the Arp2/3 complex and regulates cell migration. Nat. Cell Biol. *8*, 1383–1388.